

# Stages in the Modification of a Silver Surface for Catalysis of the Partial Oxidation of Ethylene

## I. Action of Oxygen

V. I. Bukhtiyarov, A. I. Boronin, and V. I. Savchenko

*Borokov Institute of Catalysis, Lavrentieva Prospekt 5, Novosibirsk 630090, Russia*

Received August 16, 1991; revised April 11, 1994

The interaction of silver foil with oxygen over a wide range of temperatures and O<sub>2</sub> pressures has been studied by XPS, TPD, and TPR. It has been shown that depending on the treatment conditions two adsorbed oxygen states with a different ionicity of the Ag–O bond can be formed, as well as oxygen dissolved in the silver bulk. “Ionic” oxygen [ $E_b(\text{O } 1s) = 528.4 \text{ eV}$ ] is formed in the initial step of O<sub>2</sub> adsorption, its incorporation into uppermost silver layer proceeding at  $T > 420 \text{ K}$ . This state is responsible for ethylene adsorption, followed by its destruction and complete oxidation to CO<sub>2</sub> and H<sub>2</sub>O. Dissolution of oxygen atoms in the silver bulk starts at  $T > 470 \text{ K}$ . No effect of the dissolved oxygen on the electronic and catalytic properties of the “ionic” oxygen has been revealed. Accumulation of “covalent” oxygen [ $E_b(\text{O } 1s) = 530.5 \text{ eV}$ ] occurs at higher temperature and pressure. A possible mechanism for its formation which includes the creation of specific defective sites on silver surface is discussed. Despite a large variation of pressures and temperatures used for the modification of clean silver foil by O<sub>2</sub>, all attempts to produce a surface active in ethylene epoxidation have failed. © 1994 Academic Press, Inc.

### 1. INTRODUCTION

The partial oxidation of ethylene on silver is still attracting the attention of many researchers (1–7). Despite a great number of papers, the structure of the sites active for selective oxidation on silver remains an open question. This failure seems to be determined by the gap between the pressure of the real catalytic process ( $>10^5 \text{ Pa}$ ) and the pressure at which it can be studied by surface science techniques ( $<10^{-4} \text{ Pa}$ ). The importance of high pressure is emphasized by the fact that the clean silver used in surface science studies is inactive in the ethylene oxide formation and modification under severe conditions is necessary to activate it (1–6).

One of the most promising approaches is the integration in a single ultrahigh-vacuum system of both the preliminary treatment at high pressures and the subsequent spectroscopic analysis of surface composition, followed even-

tually by testing the ethylene oxidation activity. Such methodology has been used for this system in several studies (1–4, 7).

The purpose of our work is to trace the stages of Ag modification which result finally in the formation of a catalytic centre on the silver surface that is active in the epoxidation of ethylene. In this paper, we will present data on the interaction of a silver surface with oxygen over a wide range of temperatures (420–820 K) and pressures ( $10^{-4}$ – $10^2 \text{ Pa}$ ).

### 2. EXPERIMENTAL

All the experiments were carried out with a VG ESCALAB High Pressure electron spectrometer. This spectrometer has been described earlier (8, 9). The main advantage consists in its ability to record XPS spectra *in situ* at pressures up to 1 Pa. Treatments at “high pressures” ( $P > 1 \text{ Pa}$ ) were performed in the preparation chamber. The subsequent cooling of the sample (to  $T = 420 \text{ K}$ ), its evacuation and transfer into the analyser chamber take about 3 min. The temperature of 420 K has been chosen because it is high enough to prevent the formation of carbonates (from the interaction of adsorbed oxygen with background gases) and low enough for the adlayers of oxygen to be stable (see below).

The polycrystalline silver foil (99.99%, polished by diamond paste) was fixed to a specially constructed holder designed in our Institute. This holder has independent heating of the sample for temperature programming at a wide range of heating rates and a system for rapid sample cooling with the circulation of either cold water or liquid nitrogen. The temperature of the sample was measured by a Pt–Pt/Rh thermocouple welded to the back of the Ag foil. This construction enables us to apply electron spectroscopy and thermodesorption mass spectroscopy together.

Temperature-programmed desorption (TPD) and tem-

perature-programmed reaction (TPR) spectra were recorded with a quadrupole mass spectrometer VG Q7/B and a heating rate of  $10 \text{ K s}^{-1}$ . The procedure of measuring TPR spectra was as follows: first, adsorption of ethylene for 10 min at  $T = 300 \text{ K}$  and  $P = 10 \text{ Pa}$ ; second, heating the sample, simultaneously recording TPR spectra of  $\text{CO}_2$  ( $m/z = 44$ ) and  $\text{C}_2\text{H}_4\text{O}$  ( $m/z = 29$ ). We also monitored the masses characteristic of  $\text{C}_2\text{H}_4$  ( $m/z = 27$ ),  $\text{CO}$  ( $m/z = 28$ ), and  $\text{O}_2$  ( $m/z = 32$ ).

X-ray photoelectron spectra (XPS) were recorded using Mg  $K\alpha$  irradiation and calibrated against  $E_b(\text{Ag } 3d_{5/2}) = 368.1 \text{ eV}$ . Angle-resolved XPS was achieved by turning the sample holder. This changes the XPS analysis depth according to the equation

$$d = \lambda_e \cos \Theta,$$

where  $\lambda_e$  is the mean free path of photoelectrons in the solid and  $\Theta$  is the take-off angle measured from the normal of the surface (10). The angular dependence of relative SPX intensities has proved to be very sensitive to the structure of adsorbed layers (10–12).

Silver cleaning was performed both by severe redox treatments with  $\text{O}_2$  and  $\text{H}_2$  ( $T = 670 \text{ K}$  and  $P = 5 \text{ kPa}$ ) and cycles of ionic etching followed by  $\text{O}_2$  adsorption and flashing in vacuum up to  $900 \text{ K}$ . This cycle of cleaning and recording of XPS spectra with high sensitivity was performed before every experiment to control contamination. Note that even with such severe cleaning a broad low intensity peak with  $E_b \approx 533 \text{ eV}$  was always registered in the  $\text{O } 1s$  spectra. Other authors (13, 14) have also detected small amounts of background oxygen which could not be removed up to very high temperatures. This effect seems to be related to the presence of defective sites on

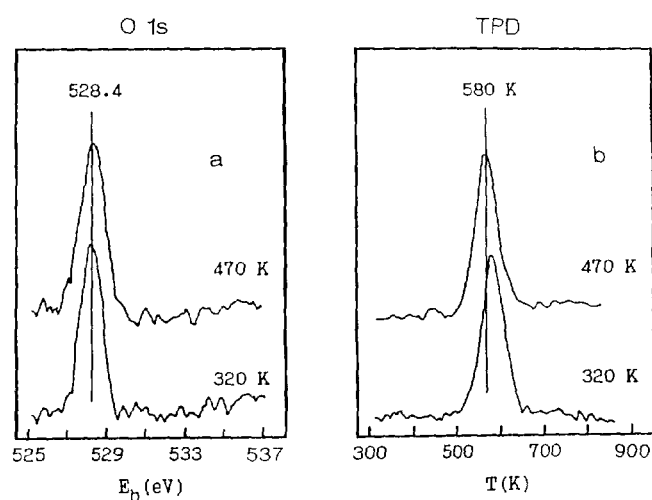


FIG. 1. (a)  $\text{O } 1s$  spectra and (b) TPD spectra of  $\text{O}_2$  after oxygen adsorption on clean silver at  $P = 10^{-2} \text{ Pa}$  and  $T = 320$  and  $470 \text{ K}$ .

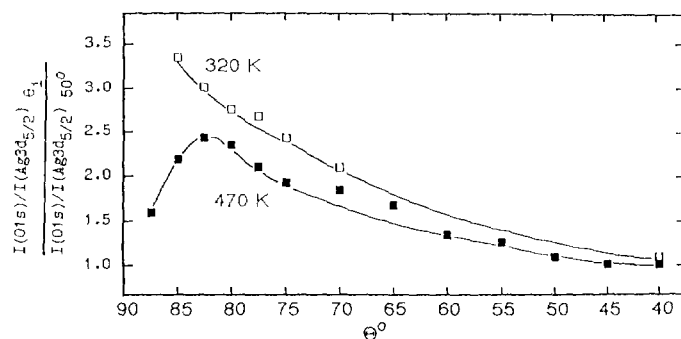


FIG. 2. Variation in  $\text{O } 1s$  and  $\text{Ag } 3d_{5/2}$  intensity ratio with take-off angle of photoelectrons ( $\Theta$ ) measured after oxygen adsorption at  $P = 10^{-2} \text{ Pa}$  and  $T = 320 \text{ K}$  ( $\square$ ) and  $470 \text{ K}$  ( $\blacksquare$ ). All ratios were normalized to those for  $\Theta = 50^\circ$ .

the polycrystalline surface, since no background oxygen has been revealed in our later work with  $\text{Ag}(111)$  single crystal. Therefore, all  $\text{O } 1s$  data are presented as difference spectra. It should be noted that this oxygen state (10% coverage from monolayer) does not influence the adsorption probability of the prepared silver surface.

Surface concentrations have been estimated by measuring the area ( $S$ ) of the  $\text{O } 1s$  and  $\text{Ag } 3d_{5/2}$  peaks, and using the fact that the  $\text{O } 1s/\text{Ir } 4f_{7/2}$  ratio (0.078) (15) corresponds to the  $\text{Ir}(111) - (2\sqrt{3} \times 2\sqrt{3}) R30^\circ\text{-CO}$  LEED pattern (16), i.e., ca.  $9.1 \times 10^{18} \text{ atoms/m}^2$ , and the  $\text{Ir } 4f_{7/2}$  and  $\text{Ag } 3d_{5/2}$  atomic sensitivity factors from Ref. (17):

$$N(\text{O}) = 2.2 \cdot 10^{20} \times S(\text{O } 1s)/S(\text{Ag } 3d_{5/2}) \text{ atoms/m}^2.$$

An analogous equation may be obtained from the  $\text{O}_2/\text{Cu}(110)$  data of Braithwaite *et al.* (18).

### 3. RESULTS

#### 3.1. Oxygen Adsorption at $T \leq 470 \text{ K}$

This range of temperature and pressure was chosen to study in detail the initial step of  $\text{O}_2$  action on silver and also to afford comparisons with literature data.

Figure 1 shows (a)  $\text{O } 1s$  spectra and (b) TPD spectra of  $\text{O}_2$  after oxygen adsorption on the clean silver surface at  $T = 320$  and  $470 \text{ K}$ , and  $P = 10^{-2} \text{ Pa}$ . One can see that for both temperatures a line appears in the  $\text{O } 1s$  region with  $E_b(\text{O } 1s) = 528.4 \text{ eV}$  and the TPD spectra are characterized by a peak with  $T_{\text{max}} \approx 580 \text{ K}$ . This oxygen state reaches saturation ( $N = 4.0 - 4.5 \times 10^{18} \text{ atoms/m}^2$ ) at an exposure of  $10^{-2} \text{ Pa}$  for 5 min. This allows us to estimate the oxygen sticking probability as  $\approx 10^{-3}$  (19, 20). Increasing the oxygen pressure up to  $100 \text{ Pa}$  does not change the shape and intensity of the spectra.

Figure 2 presents the variation of  $\text{O } 1s$  and  $\text{Ag } 3d_{5/2}$  intensity ratios with the take-off angle of photoelectron

emission measured after  $O_2$  adsorption both at 320 and at 470 K. A constant growth of the ratio with increasing  $\Theta$  is observed after oxygen adsorption at 320 K, while the adsorption of  $O_2$  at  $T = 470$  K results in a maximum in the ratio (Fig. 2). The former curve is characteristic of an adsorbate located at the surface (10–12), whereas the latter case suggests penetration of the oxygen atoms under the uppermost silver layer. Indeed, the use of grazing angles ( $\Theta > 80^\circ$ ) decreases the XPS analysis depth to a few Å (see Experimental) where the uppermost, surface layer gives the main contribution to the total XPS signal. The absence of oxygen atoms in this layer gives rise to a decrease in the oxygen intensity and, hence, a decrease in the measured ratio  $I(O\ 1s)/(Ag\ 3d_{5/2})$ . Quantitative confirmation of the oxygen incorporation follows from depth concentration profile restoration of these ARXPS data (12).

Thus, an increase of adsorption temperature from 320 to 470 K changes sharply the location of oxygen atoms with respect to the upper silver layers. However, this is not accompanied by changes in the spectral characteristics of oxygen. One can observe only some broadening of the O 1s line from 1.3 to 1.6 eV and a slight decrease in the  $T_{max}$  of the TPD peak of  $O_2$  (Fig. 1).

The reactivity of this state of  $O_{ads}$  towards  $C_2H_4$  was tested under non-steady-state conditions by TPR. Figure 3 shows (a) O 1s spectra before and after ethylene adsorption, as well as (b) TPR spectra of  $CO_2$  and  $C_2H_4O$ . It is seen that ethylene adsorption changes the electronic state of  $O_{ads}$ , while the subsequent heating of coadsorbed layers results in the formation and desorption of  $CO_2$  only (Fig. 3). Variation in the surface coverage of this  $O_{ads}$  changes

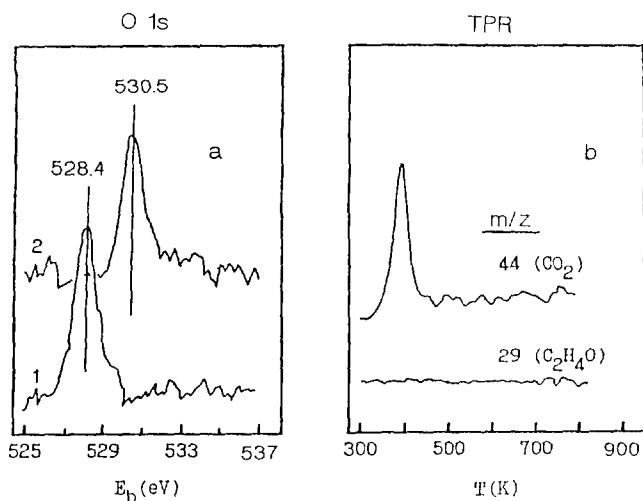


FIG. 3. (a) O 1s spectrum (2) and (b) TPD spectra of  $CO_2$  and  $C_2H_4O$  after ethylene adsorption at  $P = 10$  Pa and  $T = 300$  K on silver surface containing  $O_{ads}$  with  $E_b(O\ 1s) = 528.4$  eV (1).

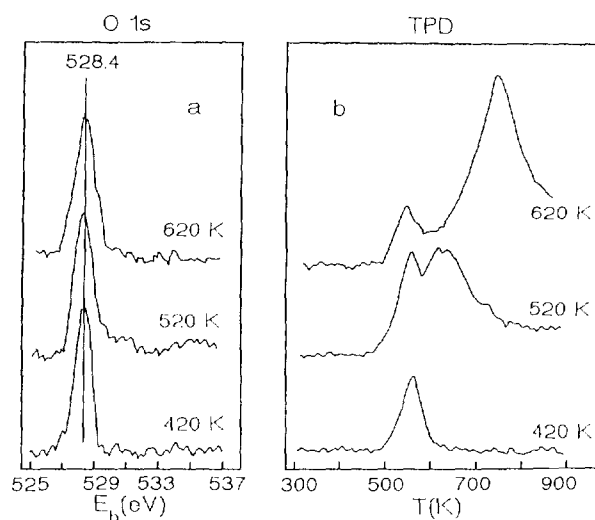


FIG. 4. (a) O 1s spectra and (b) TPD spectra  $O_2$  for silver treated by  $O_2$  for 30 min at  $P = 100$  Pa and various temperatures.

only the quantity of  $CO_2$  desorbing into the gas phase; i.e., this oxygen state is active only in the reaction of complete oxidation. Similar results were obtained for both temperatures of adsorption studied.

### 3.2. $O_2$ Interaction with the Silver at $T > 470$ K

Figure 4 presents (a) O 1s spectra and (b) TPD spectra (profiles) of  $O_2$  recorded after treatment of the silver by  $O_2$  for 30 min at  $P = 100$  Pa and elevated temperatures. The corresponding spectra recorded after  $O_2$  adsorption at  $T = 420$  K are shown for comparison. One can see that unlike the situation at low  $T$  (Fig. 4b, curve 1), an increase of  $P(O_2)$  at higher temperatures enhances the quantity of desorbing oxygen (Fig. 4b, curves 2, 3). However, the form of the O 1s spectra, as well as the oxygen concentration measured by XPS, remains constant (Fig. 4a, curves 2, 3). These data indicate that at  $T > 470$  K and high  $P(O_2)$ , oxygen dissolution in the silver bulk is occurring.

Ethylene oxidation over a silver sample with a substantial quantity of dissolved oxygen in the bulk shows that, like the clean surface (Fig. 3), the reaction route is determined by the oxygen state with  $E_b(O\ 1s) = 528.4$  eV. The latter, even in the presence of dissolved oxygen, is active only in complete oxidation of ethylene.

Severe treatment of the silver by  $O_2$  provides not only oxygen dissolution into the metal bulk but also the appearance of a new state of  $O_{ads}$  with  $E_b(O\ 1s) = 530.5$  eV. The formation of this oxygen state is quite a slow process and depends on both the  $O_2$  pressure and the silver temperature.

Figure 5 shows O 1s spectra recorded after oxygen adsorption at (a)  $P = 10^{-1}$  Pa and (b)  $P = 100$  Pa, and different temperatures. Each spectrum was recorded after

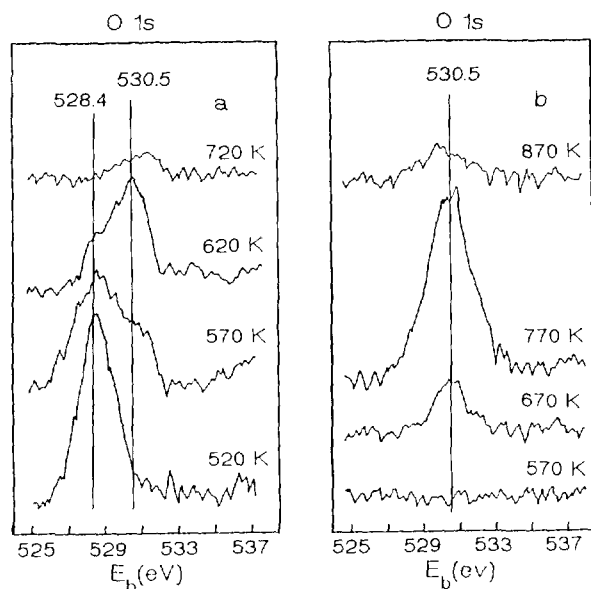


FIG. 5. O 1s spectra for silver treated by O<sub>2</sub> for 30 min at (a)  $P = 10^{-1}$  and (b) 100 Pa and various temperatures.

30 min treatment of the clean Ag surface at the chosen  $T$  and  $P$ . Note that, unlike the spectra of Fig. 5a recorded *in situ*, the O 1s spectra of Fig. 5b were recorded after the following procedure: first, cooling the sample down to 420 K followed by spectrometer evacuation (see Experimental); second, a rapid flashing in vacuum up to  $T = 600$  K for the desorption of O<sub>ads</sub> with  $E_b(\text{O } 1s) = 528.4$  eV. This heating of the sample was necessary in order to exclude uncertainty in the concentration of the latter which could appear both at the conditions of the treatment and during the sample cooling. Therefore, the O 1s spectra shown in Fig. 5b do not contain information about oxygen with  $E_b(\text{O } 1s) = 528.4$  eV.

From Fig. 5a, it is seen that an increase of the adsorption temperature higher than 520 K results in the appearance of a line with  $E_b(\text{O } 1s) = 530.5$  eV. The concentration profile of this oxygen with temperature has a maximum: at  $T > 620$  K its quantity starts to decrease and becomes negligible at  $T > 720$  K. A similar effect is also observed after O<sub>2</sub> adsorption at higher pressure (Fig. 5b), but the maximum is shifted to higher temperatures by about 150 K. The dependences of the concentration of O<sub>ads</sub> with  $E_b(\text{O } 1s) = 530.5$  eV on the temperature calculated from the data of Fig. 5 support this observation quantitatively (Fig. 6). Indeed, the increase of oxygen pressure shifts the formation of the new state of O<sub>ads</sub> to higher temperatures ( $T > 620$  K). We could not measure the TPD characteristics of this oxygen, since its formation was accompanied by oxygen dissolution into the silver bulk (compare Fig. 4 and Fig. 5). The large quantity of the dissolved oxygen (Fig. 4) screens a possible TPD peak of the new

O<sub>ads</sub>. However, the data presented in Fig. 5 shows that this oxygen has a higher desorption temperature than O<sub>ads</sub> with  $E_b(\text{O } 1s) = 528.4$  eV.

As with the two previous cases the reactivity of this state towards C<sub>2</sub>H<sub>4</sub> was checked. The silver surface containing only O<sub>ads</sub> with  $E_b(\text{O } 1s) = 530.5$  eV does not adsorb ethylene. Taking into account that the state with  $E_b(\text{O } 1s) = 528.4$  eV generates chemisorption of ethylene (Fig. 3), a test on the cooperative effect of the two oxygen states was performed. However, as in the earlier experiments (Fig. 3), only the complete oxidation product (CO<sub>2</sub>) was observed in the TPR spectra. The intensity of the TPR peak of CO<sub>2</sub> was determined by the concentration of the oxygen with  $E_b(\text{O } 1s) = 528.4$  eV.

#### 4. DISCUSSION

##### 4.1. O<sub>2</sub> Adsorption, Initial Stages

O<sub>2</sub> adsorption initially results in the formation of an oxygen state with the following characteristics:  $E_b(\text{O } 1s) = 528.4$  eV,  $T_{\text{max}}^{\text{des}} = 580$  K, and  $S_0 \approx 10^{-3}$ . Such characteristics have been observed many times both in our work (7, 9) and in the papers of other authors (19–28), indicating the appearance of adsorbed atomic oxygen. To determine the surface coverage of this oxygen it is necessary to know the number of silver atoms in the surface layer, which is not a straightforward matter for a polycrystalline sample. However, the value of the oxygen sticking probability, namely  $10^{-3}$ , which is much higher than that for Ag(111) single crystal, namely,  $10^{-6}$  (20), allows us to suggest that the surface of the silver studied contains more open planes. This suggestion is confirmed by X-ray diffraction phase analysis, with which we have measured the percentage of different types of planes present in our sample. The (110) plane appears to give the predominant contribution ( $\approx 70\%$ ). Taking into account that the concentration of Ag surface atoms for this plane is  $8.4 \times 10^{18}$  atoms/m<sup>2</sup>, the estimated coverage ( $\theta$ ) is about 0.5.

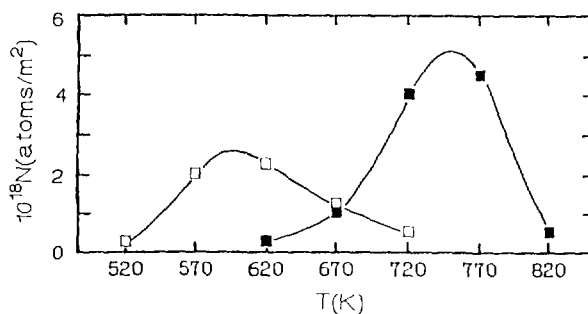


FIG. 6. Variation in concentration of O<sub>ads</sub> with  $E_b(\text{O } 1s) = 530.5$  eV with temperature for silver treated by O<sub>2</sub> for 30 min at  $P = 10^{-1}$  Pa (□) and 100 Pa (■).

The electronic properties of this oxygen state have been discussed in a number of works (19–22, 28). Thus, the oxide nature of oxygen adsorbed on silver was noted by Bowker (28) based on the coincidence of the  $T_{\text{max}}^{\text{des}}$  value for adsorbed oxygen and for the bulk oxide  $\text{Ag}_2\text{O}$ . The high ionicity of the bond of this state with silver atoms is also assumed in Refs. (19, 25). Moreover, the formation of surface ordered  $\text{Ag}_2\text{O}$  at  $T = 470$  K was concluded in other papers (20, 22) for the explanation of LEED data.

Experimental data obtained both in our present and previous work are in agreement with the conclusion about the formation of silver surface oxide. It has been shown that the formation of the oxygen with  $E_{\text{b}}(\text{O } 1s) = 528.4$  eV is accompanied by the appearance of a new component in Ag  $3d_{5/2}$  spectra with  $E_{\text{b}} = 367.7$  eV (29), approximately 0.5 eV lower than for metallic Ag (368.1 eV). The coincidence of this value with that measured for silver oxides (30) testifies the formation of ions of  $\text{Ag}^+$ . The ethylene adsorption on this surface (Fig. 3) also confirms the existence of the  $\text{Ag}^+$  (31). Taking into account the oxygen saturation coverage  $\theta \sim 0.5$ , one can conclude that the formation of surface oxide with composition of  $\text{Ag}_2\text{O}$  occurs. This oxide is unlikely to be formed at temperatures just above room temperature, since oxygen adsorption at  $T = 320$  K proceeds without changing the initial structure of the silver surface. The incorporation of oxygen atoms under the uppermost silver layer with a raising of the adsorption temperature is likely to reflect the formation of an ordered phase of surface silver oxide.

Despite the change in location with respect to the upper silver layers, the ionicity of the Ag–O bond for this oxygen remains high and that determines its activity in the total oxidation only. This result is in accordance with the data of van Santen *et al.* (32), who have shown that “ionic” oxygen is preferable for the nucleophilic attack of ethylene, with the cleavage of the C–H bond in the ethylene molecule being the first step in the complete oxidation. Nevertheless, its role in this reaction is very important and will be discussed further.

#### 4.2. Oxygen Dissolution into the Silver Bulk

Simultaneous application of XPS and TPD (see Experimental) allowed us to show that the severe treatment of the silver by  $\text{O}_2$  at high  $T$  and  $P$  results in the dissolution of oxygen into the metal bulk (Fig. 3). A high temperature TPD peak of  $\text{O}_2$  assigned to dissolved oxygen was first revealed by Rovida *et al.* both on Ag(111) (21) and on Ag(110) (22) single crystals. Afterwards, a number of authors have observed the dissolution of oxygen atoms into silver (6, 33) at high temperatures. Thus, the process of oxygen dissolution seems to be a general property of silver both for single crystals and for polycrystalline samples.

The absence of any XPS signal for the dissolved oxygen

can be explained in two ways: first, the oxygen atoms are located deeper than the XPS analysis depth ( $\approx 20$  Å) or, second, their concentration in each metal layer is lower than the XPS sensitivity level. Based only on our data we are not able to distinguish between these explanations. However, it is clear that the small quantities of oxygen in subsurface silver layers do not influence the ionicity of the adsorbed oxygen. It remains high and results in the total oxidation of ethylene. Thus, the dissolution of oxygen in quantities of more than a few monolayers does not change the route of the ethylene epoxidation compared with the clean surface, although we cannot exclude its influence under more severe conditions.

#### 4.3. Formation of Oxygen with $E_{\text{b}}(\text{O } 1s) = 530.5$ eV

The interaction of silver with  $\text{O}_2$  at high temperatures results not only in the dissolution of oxygen atoms in the metal bulk, but also in the formation of another oxygen state with  $E_{\text{b}}(\text{O } 1s) = 530.5$  eV. The appearance of new oxygen states with  $E_{\text{b}}(\text{O } 1s) = 529.0$  and 530.3 eV at high temperatures and pressures of  $\text{O}_2$  has also been revealed by Bao *et al.* (34), who have studied oxygen interaction with Ag(111) single crystal by XPS and Raman spectroscopy. They have suggested that the latter peak refers to bulk oxygen; however, our data contradict this assignment. Comparison of the TPD and XPS data presented in Figs. 4 and 6 indicates that the dissolution of oxygen and the formation of the “covalent” oxygen seem to be independent processes. Indeed,  $T = 520$  K is high enough for the efficient dissolution of oxygen atoms into the silver bulk (Fig. 4), but no “covalent” oxygen signal is registered in the O  $1s$  spectra (Fig. 6). Furthermore, raising the pressure at 620 K decreases the amount of the “covalent” oxygen (Fig. 6) despite an increase in the intensity of the desorption peak corresponding to the dissolved oxygen. Thus, the state with  $E_{\text{b}}(\text{O } 1s) = 530.5$  eV seems to be adsorbed oxygen. Our failure to register the oxygen state with  $E_{\text{b}}(\text{O } 1s) = 529.0$  eV can be explained either by the lower pressures of  $\text{O}_2$  used in the present work or by the fact that our surface is more open than the (111) plane used by Bao *et al.* (34). Indeed, the same authors (35) have shown that the oxygen interaction with the more open (110) silver plane provides only one peak in the Raman spectrum at  $630\text{ cm}^{-1}$  which corresponds to  $\text{O}_{\text{ads}}$  with  $E_{\text{b}}(\text{O } 1s) = 530.3$  eV.

The increase in the O  $1s$  binding energy (from 528.4 to 530.5 eV), the absence both of an ionic component in the Ag  $3d_{5/2}$  spectra at its formation and of any adsorption of ethylene at the pressure studied testify to a decrease in the negative charge on this  $\text{O}_{\text{ads}}$  compared with that of the “ionic” oxygen. Since no substantial transfer of electronic density from the silver atoms to this oxygen seems to occur, we use the term “covalent” in order to underline

the low ionicity of its Ag–O bond compared with that in the surface oxide.

The sharp increase in the covalency of adsorbed oxygen is most likely to be determined by the creation of some defective sites with structure different from that of the clean silver surface. These structural changes occur under the influence of O<sub>2</sub> in the gas phase, since no "covalent" O<sub>ads</sub> appears after oxygen adsorption on a silver surface annealed for a few hours at high temperatures in vacuum. As follows from the data presented, two processes proceed with high efficiency in these conditions: first, the formation and removal (desorption) of the "ionic" oxygen and, second, the dissolution of oxygen atoms into the silver bulk. The absence of any correlation between the "covalent" O<sub>ads</sub> and dissolved oxygen allows us to choose the former process. Indeed, adsorption and desorption of the "ionic" oxygen cause the reverse transformation of the initial structure of the clean surface to the structure of surface oxide, many repetitions of which provide effective mass transfer of silver atoms at the surface necessary for the creation of the defective sites mentioned above. These defective sites unstable in vacuum at high temperatures can be stabilized by the formation of a bond with adsorbed oxygen. Such processes resulting in the microfaceting of surfaces has been revealed for the CO + O<sub>2</sub>/Pt(110) system (36). We believe that these defective sites are responsible for the formation of the "covalent" oxygen in our case, although additional experiments are necessary to elucidate the mechanism.

In conclusion, it should be noted that despite great variation of the pressures and temperatures used for modification of clean silver foil by pure O<sub>2</sub>, all attempts to produce a surface active in ethylene epoxidation have failed. Neither the incorporation of oxygen atoms into the uppermost silver layer nor the formation of large amounts of dissolved oxygen changes the electronic properties of the "ionic" oxygen [ $E_b(\text{O } 1s) = 528.4 \text{ eV}$ ], which is active only in the total combustion of ethylene. Moreover, even the formation of a new adsorbed oxygen state with a more covalent character of the Ag–O bond [ $E_b(\text{O } 1s) = 530.5 \text{ eV}$ ] does not give rise to ethylene oxide amongst the reaction products. Apparently, modification by the reaction mixture is necessary for the activation of clean silver in ethylene epoxidation.

#### ACKNOWLEDGMENTS

We are very grateful to S. V. Bogdanov for the X-ray diffraction measurements and to I. P. Prosvirin for technical assistance.

#### REFERENCES

1. Backx, C., Moolhuysen, J., Geenen, P., and van Santen, R. A., *J. Catal.* **72**, 364 (1981).
2. van Santen, R. A., and de Groot, C. P. M., *J. Catal.* **98**, 530 (1986).
3. Parfenov, A. N., Avetisov, A. K., and Gelbstein, A. I., *Dokl. Akad. Nauk SSSR* **272**, 1168 (1983). [In Russian]
4. Grant, R. B., and Lambert, R. M., *J. Catal.* **92**, 364 (1985).
5. Campbell, C. T., and Paffett, M. T., *Surf. Sci.* **139**, 396 (1984).
6. Haul, R., and Neubauer, G., *J. Catal.* **105**, 39 (1987).
7. Bukhtiyarov, V. I., Boronin, A. I., and Savchenko, V. I., *Surf. Sci.* **232**, L205 (1990).
8. Joyner, R. W., Roberts, M. W., and Yates, K., *Surf. Sci.* **87**, 501 (1979).
9. Boronin, A. I., Bukhtiyarov, V. I., Vishenskii, A. L., Borekov, G. K., and Savchenko, V. I., *Surf. Sci.* **201**, 195 (1988).
10. Fadley, C. S., Baird, R. J., Siekhaus, W., Novakov T., and Bergstrom, S. A. L., *J. Electron Spectrosc. Relat. Phenom.* **4**, 93 (1974).
11. Boronin, A. I., *Bulg. Chem. Commun.* **22**, 178 (1989).
12. Baschenko, O. A., Bukhtiyarov, V. I., and Boronin, A. I., *Surf. Sci.* **271**, 493 (1992).
13. Grimblot, J., Alnot, P., Behm, R. J., and Brundle, C. R., *J. Electron Spectrosc. Relat. Phenom.* **52**, 175 (1990).
14. Lefferts, L., van Ommen, J. G., and Ross, J. R. H., *J. Chem. Soc. Faraday Trans. 1* **83**, 161 (1987).
15. Boronin, A. I., Ph.D. thesis, Novosibirsk, 1983. [In Russian]
16. Ivanov, V. P., Borekov, G. K., and Savchenko, V. I., *J. Catal.* **48**, 269 (1977).
17. Wagner, C. D., Davies, L. E., Zeller, M. V., Tavior, J. A., Raymond, R. H., and Gale, L., *Surf. Interface Anal.* **3**, 211 (1981).
18. Braithwaite, M. J., Joyner, R. W., and Roberts, M. W., *J. Chem. Soc. Faraday Trans. 1* **60**, 89 (1975).
19. Campbell, C. T., and Paffett, M. T., *Surf. Sci.* **143**, 517 (1984).
20. Campbell, C. T., *Surf. Sci.* **157**, 43 (1985).
21. Rovida, G., Pratesi, F., Maglietta, M., and Ferroni, E., *Surf. Sci.* **43**, 230 (1974).
22. Rovida, G., and Pratesi, F., *Surf. Sci.* **52**, 542 (1975).
23. Englehardt, H. A., and Menzel, D., *Surf. Sci.* **57**, 591 (1976).
24. Backx, C., de Groot, C. P. M., Biloen, R., and Sachtler, W. M. H., *Surf. Sci.* **128**, 81 (1981).
25. Barteau, M. A., and Madix, R. J., *J. Electron Spectrosc. Relat. Phenom.* **31**, 101 (1983).
26. Grant, R. B., and Lambert, R. M., *Surf. Sci.* **146**, 256 (1984).
27. Bowker, M., *Vacuum* **33**, 699 (1983).
28. Bowker, M., *Surf. Sci.* **155**, L276 (1985).
29. Bukhtiyarov, V. I., and Boronin, A. I., in "Proceedings, Russian Conference on the Study of Catalysts by Electron and Ion Spectroscopy. Omsk, Omsk Division of the Institute of Catalysis, 1992," p. 56. [In Russian]
30. Hammond, J. S., Gaarenstrom, S. W., and Winograd, N., *Anal. Chem.* **47**, 2193 (1975).
31. Campbell, C. T., and Paffett, M. T., *Appl. Surf. Sci.* **19**, 28 (1984).
32. van Santen, R. A., Moolhuysen, S., and Sachtler, W. M. H., *J. Catal.* **65**, 478 (1980).
33. Rehren, C., Isaac, G., Schlögl, R., and Ertl, G., *Catal. Lett.* **11**, 253 (1991).
34. Bao, X., Muhler, M., Pettinger, B., Schlögl, R., and Ertl, G., *Catal. Lett.* **22**, 215 (1993).
35. Bao, X., Pettinger, B., Ertl, G., and Schlögl, R., *Ber. Bunsenges. Phys. Chem.* **97**, 322 (1993).
36. Imbihl, R., Sander, M., and Ertl, G., *Surf. Sci.* **204**, L701 (1988).